crystals

MDPI

Communication

Aurophilic Interactions in Cationic Three-Coordinate Gold(I) Bipyridyl/Isocyanide Complex

Mariya V. Grudova [1], Alexander S. Novikov [2], Alexey S. Kubasov [3], Victor N. Khrustalev [1,4], Anatoly A. Kirichuk [1], Valentine G. Nenajdenko [5] and Alexander G. Tskhovrebov [1,6,*]

1 Research Institute of Chemistry, Peoples' Friendship University of Russia, 6 Miklukho-Maklaya Street, 117198 Moscow, Russia; shokoi@mail.ru (M.V.G.); vnkhrustalev@gmail.com (V.N.K.); kirichuk-aa@rudn.ru (A.A.K.)
2 Institute of Chemistry, Saint Petersburg State University, Universitetskaya Nab. 7/9, 199034 Saint Petersburg, Russia; a.s.novikov@spbu.ru
3 Kurnakov Institute of General and Inorganic Chemistry, Russian Academy of Sciences, Leninsky Prosp. 31, 119071 Moscow, Russia; fobosax@mail.ru
4 N.D. Zelinsky Institute of Organic Chemistry, Russian Academy of Sciences, 47 Leninsky Prosp., 119334 Moscow, Russia
5 Department of Chemistry, M. V. Lomonosov Moscow State University, 1, Leninskie Gory, 119991 Moscow, Russia; nenajdenko@gmail.com
6 N.N. Semenov Federal Research Center for Chemical Physics, Russian Academy of Sciences, Kosygina 4, 119991 Moscow, Russia
* Correspondence: tskhovrebov-ag@rudn.ru

check for updates

Citation: Grudova, M.V.; Novikov, A.S.; Kubasov, A.S.; Khrustalev, V.N.; Kirichuk, A.A.; Nenajdenko, V.G.; Tskhovrebov, A.G. Aurophilic Interactions in Cationic Three-Coordinate Gold(I) Bipyridyl/Isocyanide Complex. *Crystals* **2022**, *12*, 613. https://doi.org/10.3390/cryst12050613

Academic Editors: Jesús Sanmartín-Matalobos and Waldemar Maniukiewicz

Received: 6 April 2022
Accepted: 24 April 2022
Published: 26 April 2022

Publisher's Note: MDPI stays neutral with regard to jurisdictional claims in published maps and institutional affiliations.

Copyright: © 2022 by the authors. Licensee MDPI, Basel, Switzerland. This article is an open access article distributed under the terms and conditions of the Creative Commons Attribution (CC BY) license (https://creativecommons.org/licenses/by/4.0/).

Abstract: Gold(I) isocyanide complexes featuring Au···Au interactions attract considerable attention because of their tunable photophysical properties. Although the synthetic exploration of isocyanide gold(I) complexes seems reasonable, their structural diversity is mainly limited to linear gold(I) derivatives. The synthesis and structural characterization of cationic three-coordinate gold(I) mixed 2,2′-bipyridyl/isocyanide complex are presented here for the first time. Cationic gold species form supramolecular dimers in the solid state via attractive Au···Au interactions. The nature and energies of aurophilic contacts, which are responsible for dimerization in the solid state, were studied by DFT calculations together with QTAIM, ELF, RDG, and NCI techniques and Hirshfeld surface analysis. The estimated energy of the aurophilic interactions was 6.3 kcal/mol.

Keywords: gold; noncovalent interactions; aurophilic interactions; isocyanides

1. Introduction

Metallophilic interactions in soft materials have recently emerged as a topic of growing interest since they have an impact on material properties, such as photophysical [1,2] and magnetic properties [3], electrical conductivity [4,5], sensing [6], etc. Several reports have demonstrated that the strength of aurophilic contacts is comparable to that of hydrogen bonding [7,8].

Aurophilic interactions have been implicated in the intriguing luminescent features of metal complexes. The isocyanide complexes of gold(I) are versatile luminescent compounds that have attracted significant attention and often feature aurophilic contacts [9,10]. These attractive Au···Au interactions in isocyanide complexes are important since they influence the self-assembly of these materials in the solid state. Neutral linear aryl gold(I) isocyanide derivatives showed potential in the context of the exploration of their tunable photophysical characteristics in the solid state, which could be affected by aurophilic interactions [11–13]. Cationic linear diisocyanide gold(I) complexes also showed a propensity to self-assemble in the solid state in higher-order emissive aggregates via attractive Au···Au interactions [1,9,10]. Although the synthetic exploration of isocyanide gold(I) complexes is an attractive area, their structural diversity seems to be limited to linear gold(I)

derivatives. Here, we describe the synthesis and structural characterization of the cationic three-coordinate gold(I) 2,2′-bipyridyl/isocyanide complex, which forms supramolecular dimers in the solid state via attractive Au···Au interactions, for the first time. In addition, we performed DFT calculations together with QTAIM, ELF, RDG, and NCI techniques and Hirshfeld surface analysis, which supported the presence of intermolecular aurophilic interactions in the solid state.

2. Materials and Methods

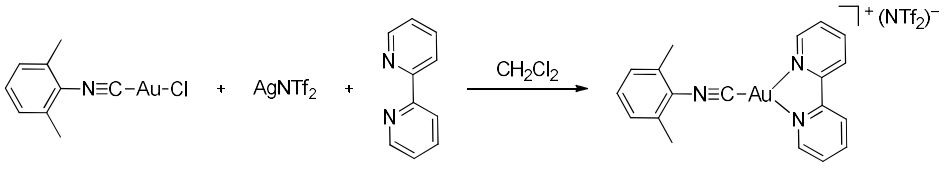
General remarks. All manipulations were carried out in air unless specified otherwise. All the chemicals employed in this work were purchased from commercial suppliers (Aldrich (Schnelldorf, Germany), TCI-Europe (Zwijndrecht, Belgium), Strem (Bischheim, France), and ABCR (Karlsruhe, Germany)). The solvents were distilled using standard methods. Nuclear magnetic resonance spectra were obtained on a Bruker Avance neo 700 (Karlsruhe, Germany); chemical shifts (δ) are given in ppm, and coupling constants (J) are given in Hz. C, H, and N elemental analyses were performed on a Euro EA 3028HT CHNS/O analyzer (Pavia, Italy).

Computational details. The quantum chemical calculations based on the X-ray geometry of **4** were carried out using the ωB97XD [14] DFT functional in the Gaussian-09 program [15]. The Douglas–Kroll–Hess 2nd order scalar relativistic calculations with the relativistic core Hamiltonian were carried out using the DZP–DKH basis sets [16,17] for all atoms. The topological analysis of the electron density distribution (quantum theory of atoms in molecules, QTAIM), reduced density gradient (RDG), electron localization function (ELF), and noncovalent interactions (NCI) analyses were performed using the Multiwfn program (version 3.7) [18]. The VMD program [19] was additionally utilized for visualization. The Cartesian atomic coordinates for the model structure are presented in Table S1 (Supplementary Materials). The Hirshfeld molecular surface was generated by the CrystalExplorer program (version 17.5) [20] using the normalized contact distance d_{norm} [21] based on Bondi's van der Waals radii [22].

Synthesis of 4. Silver bis(trifluoromethanesulfonyl)imide ($AgNTf_2$) (0.055 mmol, 22 mg) was added to a solution of chloro(2,6-dimethylphenyl isocyanide)gold(I) (0.055 mmol, 20 mg) in CH_2Cl_2 (1 mL). The reaction mixture was placed in an ultrasound bath for 20 min. After that, the reaction mixture was filtered, and then 2,2′-bipyridyl (0.055 mmol, 9 mg) was added. The solvent was evaporated to obtain a colorless solid (yield 80%, 21 mg). ^{1}H NMR (700 MHz, $CDCl_3$) δ 8.83 (d, J = 4.7 Hz, 2H, from bipy), 8.45 (d, J = 8.1 Hz, 2H, from bipy), 8.19 (t, J = 7.2 Hz, 2H, from bipy), 7.74 (s, 2H, from bipy), 7.37 (t, J = 7.7 Hz, 1H, from Xyl), 7.22 (d, J = 7.7 Hz, 2H, from Xyl), 2.52 (s, 6H, $2CH_3$). ^{13}C NMR (176 MHz, $CDCl_3$) δ 151.25, 141.34, 136.18 ($2C_{quat.}$ from Xyl), 131.29 (CH from Xyl), 128.73 (2CH from Xyl), 127.00, 124.01 ($C_{quat.}$ from Xyl), 121.03, 119.21, 29.83, 18.91 (2 CH_3). IR (ν): 2184 cm^{-1} (N≡C). MS (ESI^+), found: 484.1083 $[M–NTf_2]^+$; calculated for $C_{19}H_{17}AuN_3$: 484.1088.

3. Results and Discussion

Following our interest in the isocyanide complexes [23–30], triple CN bond activation [31–36], and noncovalent interactions [37–44], the gold(I) complex **4** was prepared in a high yield by the sequential addition of $AgNTf_2$ (**2**) and 2,2′-bipyridyl (**3**) to chloro(2,6-dimethylphenyl isocyanide)gold(I) (**1**) in CH_2Cl_2 as a solvent (Scheme 1).



Scheme 1. Synthesis of complex **4**.

The structure and purity of compound **4** were established by elemental analyses (C, H, N), high-resolution electrospray ionization mass spectrometry (ESI-MS), ^{1}H and ^{13}C NMR spectroscopies, and X-ray diffraction structural analysis. The ESI^{+} mass spectrum of **4** contained a peak corresponding to the cationic part of the complex ([M–NTf$_2$]$^{+}$) with the characteristic isotopic distribution. The IR spectrum of **4** exhibited one peak at 2184 cm^{-1} due to C≡N stretching vibration.

Compound **4** produced colorless crystals, which were suitable for analysis by single-crystal X-ray crystallography, when it was recrystallized from CH_2Cl_2 layered by hexane. The structural investigations confirmed the formation of the xylylisocyanide bipyridyl complex (Figure 1).

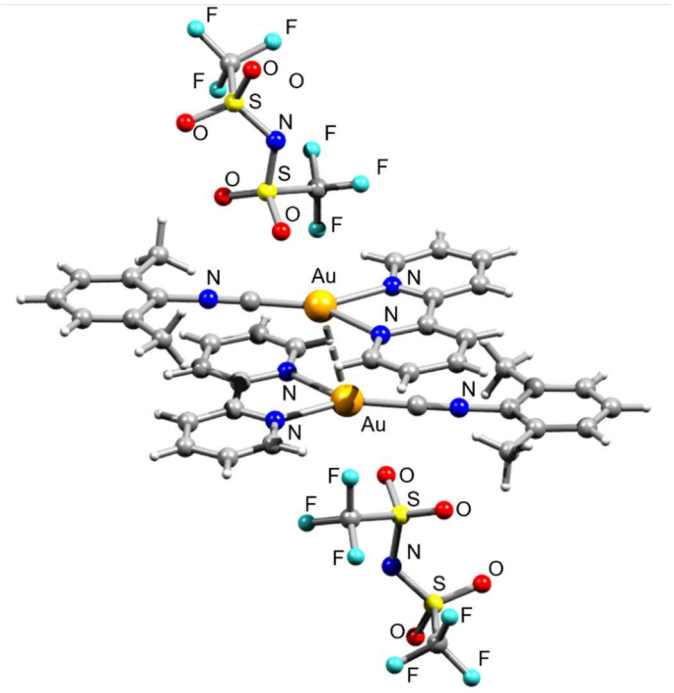


Figure 1. Ball-and-stick representation of the crystal structure of **4**, demonstrating Au· · · Au interaction. Grey and light-grey spheres represent carbon and hydrogen atoms, respectively.

The C–N–C–Au moiety in **4** is almost linear (N–C–Au and C–N–C for **1** are 178.3° and 178.1°, respectively). Interestingly, the C–Au bond distance (1.92 Å) is shorter than that of gold carbene complexes, which were described earlier [45,46]. This indicates the stronger back donation of the isocyanide to the metal center compared with the diarylcarbene ligand. Another interesting structural peculiarity of **4** is that the N–Au–C angles around the metal center are noticeably different (148.0° vs. 139.4°). The N–Au distances are also slightly different (2.26 Å vs. 2.24 Å), which means that the bypyridyl ligand is asymmetrically coordinated with the gold metal center. All other bond distances in **4** are unremarkable.

The crystallographic data analysis suggests the existence of the aurophilic interactions Au(I)···Au(I) in the crystal structure **4**. Indeed, the distance between appropriate metal centers (viz. 3.216 Å) is significantly lower than the sum of their shortest van der Waals (vdW) radii (viz. 3.32 Å; note that currently, several values of vdW radii for gold are proposed, from the "classic" 1.66 Å radii [22] to "modern" 2.32 Å radii [47]. In order to confirm or disprove the hypothesis of the existence of such intramolecular noncovalent interactions in the X-ray structure of **4**, the DFT calculations together with QTAIM, ELF, RDG, and NCI techniques [48] were carried out at the ωB97XD/DZP-DKH level of theory for the model structure (see Computational details and Table S1 in Supporting Information). The QTAIM analysis of the model structure revealed the presence of the bond critical point (3, –1) for the aurophilic interactions Au(I)···Au(I) in the X-ray structure of **4** (Figure 2 and Table 1). The values of the electron density, Laplacian of electron density, and energy density

in the bond critical point (3, –1) for the aurophilic interactions Au(I)···Au(I) in the X-ray structure of **4** are typical for metallophilic interactions in similar chemical systems [49–52]; the ratio $-G(\mathbf{r})/V(\mathbf{r}) < 1$ reveals some small covalent contribution in this short contact [53], and the sign of λ_2 ($\lambda_2 < 0$) suggests that these interactions are attractive [54,55]. The estimated energy of the aurophilic interactions Au(I)···Au(I) in **4** ($E_{int} \approx -V(\mathbf{r})/2$) [56] is 6.3 kcal/mol. The visualization of intermolecular contacts in 3D using the noncovalent interaction analysis (NCI analysis) technique and the scatter graph of RDG vs. the product of sign of λ_2 (second largest eigenvalue of the Hessian matrix of electron density) and ρ (electron density) (NCI plot [54]) for **4** are shown in Figure 3. To understand what kinds of intermolecular contacts have the largest contributions to crystal packing, we performed the Hirshfeld surface analysis for the X-ray structure of **4** (Figure 4). We found that intermolecular contacts involving hydrogen atoms (viz. H···H, C···H, O···H, and F···H) have the largest contributions to crystal packing. The fingerprint plots from the Hirshfeld surface analysis for the X-ray structure of **4** are given in the attached zip archive (Supplementary Materials).

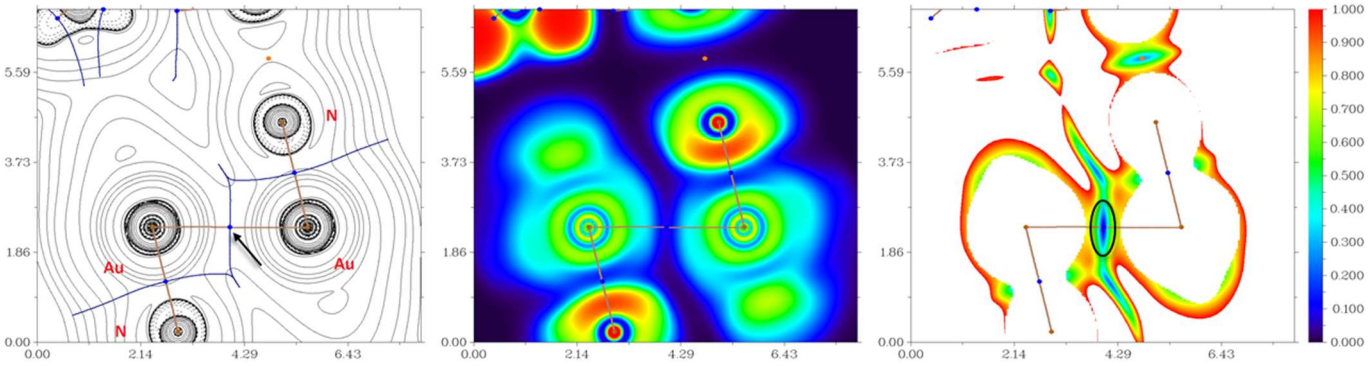


Figure 2. Laplacian of electron density distribution $\nabla^2\rho(\mathbf{r})$, visualization of electron localization function (ELF), and reduced density gradient (RDG) analyses (left, center, and right diagrams, respectively) for aurophilic interactions Au(I)···Au(I) in the X-ray structure **4**. Bond critical points (3, –1)—blue, nuclear critical points (3, –3)—pale brown, ring critical points (3, +1)—orange, bond paths—pale brown lines, length units—Å; the color scale for the ELF and RDG maps is presented in a.u. The bond critical point (3, –1) for aurophilic interactions Au(I)···Au(I) is indicated by black arrow in left diagram; the blue area of reduced density gradient, very typical for noncovalent interactions, is indicated by black ellipse in right diagram.

Table 1. The density of all electrons, ρ(**r**); Laplacian of electron density, $\nabla^2\rho(\mathbf{r})$; appropriate λ_2 eigenvalue; energy density, H_b; potential energy density, V(**r**); and Lagrangian kinetic energy, G(**r**) (a.u.) at the bond critical point (3, –1) corresponding to aurophilic interactions Au(I)···Au(I) in the X-ray structure of **4**.

ρ(**r**)	$\nabla^2\rho(\mathbf{r})$	λ_2	H_b	V(**r**)	G(**r**)
0.023	0.058	–0.023	–0.003	–0.020	0.017

In summary, we described the synthesis and structural characterization of the cationic three-coordinate gold(I) 2,2′-bipyridyl/isocyanide complex for the first time. Two cationic gold derivatives form supramolecular dimers in the crystal via attractive Au···Au contacts. The estimated energy of the aurophilic interactions in **4** is 6.3 kcal/mol.

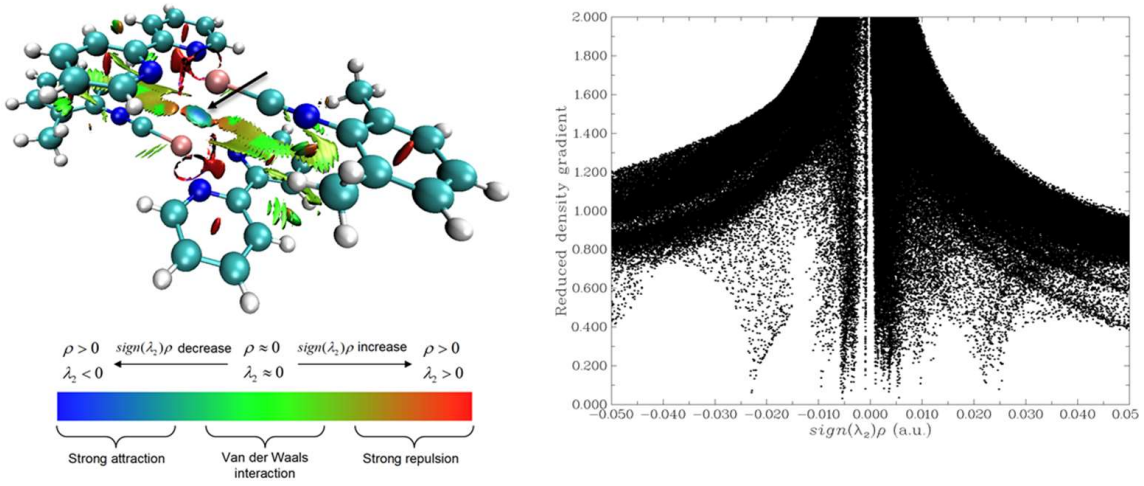


Figure 3. Visualization of intermolecular contacts in 3D using NCI analysis technique and NCI plot for **4**. Blue area responsible for attractive aurophilic interactions Au(I)···Au(I) indicated by black arrow.

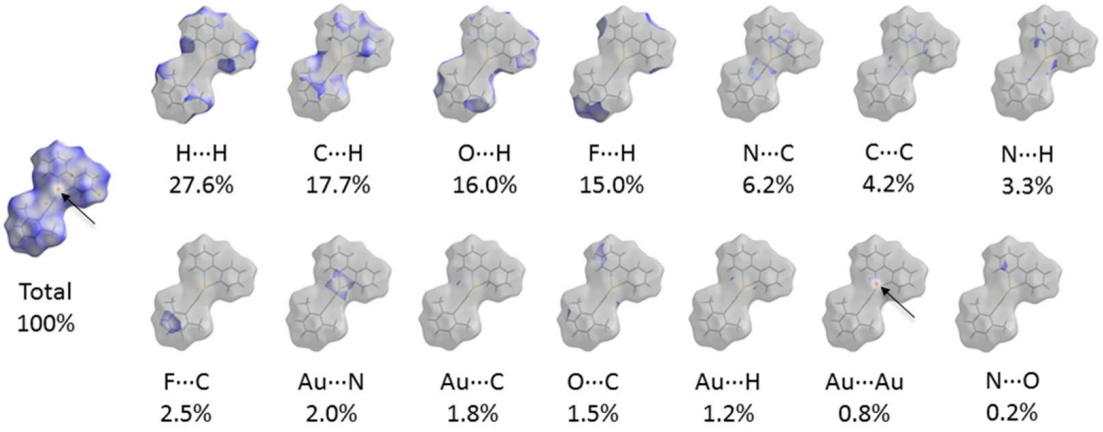


Figure 4. Visualization of Hirshfeld surface analysis for the X-ray structure of **4**. Area responsible for intermolecular contacts Au···Au (aurophilic interactions) indicated by black arrows.

Supplementary Materials: The following are available online at https://www.mdpi.com/article/10.3390/cryst12050613/s1, Table S1. Cartesian atomic coordinates for model structure of **4**, X-ray crystal structure determination, Table S2. Crystallographic parameters, data collection, and structure refinement details for X-ray structure of **4**, zip archive with fingerprint plots from Hirshfeld surface analysis for the X-ray structure of **4**. References [57–60] are cited in the supplementary materials.

Author Contributions: Conceptualization, A.G.T.; methodology, V.G.N.; software, A.S.N.; formal analysis, A.S.N. and A.S.K.; investigation, V.N.K. and M.V.G.; writing—original draft preparation, A.S.N. and A.G.T.; writing—review and editing, A.G.T.; project administration, A.A.K. All authors have read and agreed to the published version of the manuscript.

Funding: This work was supported by the RUDN University Strategic Academic Leadership Program. Funding for this research was provided by the Russian Foundation for Basic Research (project number 20-53-00006) and the Belarusian Foundation for Fundamental Research (grant X20P-066). Funding for this research was provided by the Ministry of Science and Higher Education of the Russian Federation (award no. 075-03-2020-223 (FSSF-2020-0017)).

Conflicts of Interest: The authors declare no conflict of interest.

References

1. Vickery, J.C.; Olmstead, M.M.; Fung, E.Y.; Balch, A.L. Solvent-Stimulated Luminescence from the Supramolecular Aggregation of a Trinuclear Gold(I) Complex that Displays Extensive Intermolecular Au·Au Interactions. *Angew. Chem. Int. Ed. Engl.* **1997**, *36*, 1179–1181. [CrossRef]
2. Wing-Wah Yam, V.; Kam-Wing Lo, K. Luminescent polynuclear d10 metal complexes. *Chem. Soc. Rev.* **1999**, *28*, 323–334. [CrossRef]
3. Leznoff, D.B.; Xue, B.-Y.; Stevens, C.L.; Storr, A.; Thompson, R.C.; Patrick, B.O. Synthesis, structure and magnetic properties of 3D interpenetrating nets of M(pyrazine)[Au(CN)2]2 (M=Cu, Ni, Co) supported by aurophilic interactions. *Polyhedron* **2001**, *20*, 1247–1254. [CrossRef]
4. Mitsumi, M.; Ueda, H.; Furukawa, K.; Ozawa, Y.; Toriumi, K.; Kurmoo, M. Constructing Highly Conducting Metal−Metal Bonded Solids by Electrocrystallization of [PtII2(RCS2)4] (RCS2− = Dithiocarboxylato, R = Methyl or Ethyl). *J. Am. Chem. Soc.* **2008**, *130*, 14102–14104. [CrossRef] [PubMed]
5. Guijarro, A.; Castillo, O.; Calzolari, A.; Miguel, P.J.S.; Gómez-García, C.J.; di Felice, R.; Zamora, F. Electrical Conductivity in Platinum-Dimer Columns. *Inorg. Chem.* **2008**, *47*, 9736–9738. [CrossRef] [PubMed]
6. Katz, M.J.; Ramnial, T.; Yu, H.-Z.; Leznoff, D.B. Polymorphism of Zn[Au(CN)2]2 and Its Luminescent Sensory Response to NH3 Vapor. *J. Am. Chem. Soc.* **2008**, *130*, 10662–10673. [CrossRef]
7. Schmidbaur, H.; Schier, A. A briefing on aurophilicity. *Chem. Soc. Rev.* **2008**, *37*, 1931–1951. [CrossRef]
8. Pyykkö, P. Theoretical Chemistry of Gold. *Angew. Chem. Int. Ed. Engl.* **2004**, *43*, 4412–4456. [CrossRef]
9. White-Morris, R.L.; Olmstead, M.M.; Balch, A.L. Aurophilic Interactions in Cationic Gold Complexes with Two Isocyanide Ligands. Polymorphic Yellow and Colorless Forms of [(Cyclohexyl Isocyanide)2AuI](PF6) with Distinct Luminescence. *J. Am. Chem. Soc.* **2003**, *125*, 1033–1040. [CrossRef]
10. Luong, L.M.C.; Malwitz, M.A.; Moshayedi, V.; Olmstead, M.M.; Balch, A.L. Role of Anions and Mixtures of Anions on the Thermochromism, Vapochromism, and Polymorph Formation of Luminescent Crystals of a Single Cation, [(C6H11NC)2Au]+. *J. Am. Chem. Soc.* **2020**, *142*, 5689–5701. [CrossRef]
11. Seki, T.; Sakurada, K.; Ito, H. Controlling Mechano- and Seeding-Triggered Single-Crystal-to-Single-Crystal Phase Transition: Molecular Domino with a Disconnection of Aurophilic Bonds. *Angew. Chem. Int. Ed. Engl.* **2013**, *52*, 12828–12832. [CrossRef] [PubMed]
12. Seki, T.; Kurenuma, S.; Ito, H. Luminescence Color-Tuning through Polymorph Doping: Preparation of a White-Emitting Solid from a Single Gold(I)–Isocyanide Complex by Simple Precipitation. *Chem.-A Eur. J.* **2013**, *19*, 16214–16220. [CrossRef] [PubMed]
13. Seki, T.; Kobayashi, K.; Ito, H. Low-temperature-selective luminescent mechanochromism of a thienyl gold isocyanide complex. *Chem. Commun.* **2017**, *53*, 6700–6703. [CrossRef] [PubMed]
14. Chai, J.-D.; Head-Gordon, M. Long-range corrected hybrid density functionals with damped atom–atom dispersion corrections. *Phys. Chem. Chem. Phys.* **2008**, *10*, 6615–6620. [CrossRef] [PubMed]
15. Frisch, M.J.; Trucks, G.W.; Schlegel, H.B.; Scuseria, G.E.; Robb, M.A.; Cheeseman, J.R.; Scalmani, G.; Barone, V.; Mennucci, B.; Petersson, G.A.; et al. *Gaussian 09 C.01*; Gaussian, Inc.: Wallingford, CT, USA, 2010.
16. Barros, C.L.; de Oliveira, P.J.P.; Jorge, F.E.; Canal Neto, A.; Campos, M. Gaussian basis set of double zeta quality for atoms Rb through Xe: Application in non-relativistic and relativistic calculations of atomic and molecular properties. *Mol. Phys.* **2010**, *108*, 1965–1972. [CrossRef]
17. Canal Neto, A.; Jorge, F.E. All-electron double zeta basis sets for the most fifth-row atoms: Application in DFT spectroscopic constant calculations. *Chem. Phys. Lett.* **2013**, *582*, 158–162. [CrossRef]
18. Lu, T.; Chen, F. Multiwfn: A multifunctional wavefunction analyzer. *J. Comput. Chem.* **2012**, *33*, 580–592. [CrossRef]
19. Humphrey, W.; Dalke, A.; Schulten, K. VMD: Visual molecular dynamics. *J. Mol. Graph.* **1996**, *14*, 33–38. [CrossRef]
20. Turner, M.J.; McKinnon, J.J.; Wolff, S.K.; Grimwood, D.J.; Spackman, P.R.; Jayatilaka, D.; Spackman, M.A. *CrystalExplorer17*; University of Western Australia: Crawley, WA, Australia, 2017.
21. McKinnon, J.J.; Jayatilaka, D.; Spackman, M.A. Towards quantitative analysis of intermolecular interactions with Hirshfeld surfaces. *Chem. Commun.* **2007**, *37*, 3814–3816. [CrossRef]
22. Bondi, A. Van der Waals volumes and radii of metals in covalent compounds. *J. Phys. Chem.* **1966**, *70*, 3006–3007. [CrossRef]
23. Luzyanin, K.V.; Tskhovrebov, A.G.; Guedes da Silva, M.F.C.; Haukka, M.; Pombeiro, A.J.L.; Kukushkin, V.Y. Metal-mediated [2+3] cycloaddition of nitrones to palladium-bound isonitriles. *Chem.-A Eur. J.* **2009**, *15*, 5969–5978. [CrossRef] [PubMed]
24. Tskhovrebov, A.G.; Luzyanin, K.V.; Kuznetsov, M.L.; Sorokoumov, V.N.; Balova, I.A.; Haukka, M.; Kukushkin, V.Y. Substituent R-dependent regioselectivity switch in nucleophilic addition of N-phenylbenzamidine to PdII-and PtII-complexed isonitrile RN-C giving aminocarbene-like species. *Organometallics* **2011**, *30*, 863–874. [CrossRef]
25. Tskhovrebov, A.G.; Luzyanin, K.V.; Dolgushin, F.M.; Guedes Da Silva, M.F.C.; Pombeiro, A.J.L.; Kukushkin, V.Y. Novel reactivity mode of metal diaminocarbenes: Palladium(II)-mediated coupling between acyclic diaminocarbenes and isonitriles leading to dinuclear species. *Organometallics* **2011**, *30*, 3362–3370. [CrossRef]
26. Luzyanin, K.V.; Tskhovrebov, A.G.; Carias, M.C.; Guedes da Silva, M.F.C.; Pombeiro, A.J.; Kukushkin, V.Y. Novel Metal-mediated (M = Pd, Pt) coupling between isonitriles and benzophenone hydrazone as a route to aminocarbene complexes exhibiting high catalytic activity (M = Pd) in the Suzuki-Miyaura reaction. *Organometallics* **2009**, *28*, 6559–6566. [CrossRef]

27. Mikhaylov, V.N.; Sorokoumov, V.N.; Liakhov, D.M.; Tskhovrebov, A.G.; Balova, I.A. Polystyrene-supported acyclic diaminocarbene palladium complexes in Sonogashira cross-coupling: Stability vs. catalytic activity. *Catalysts* **2018**, *8*, 141. [CrossRef]
28. Tskhovrebov, A.G.; Luzyanin, K.V.; Haukka, M.; Kukushkin, V.Y. Synthesis and characterization of cis-(RNC)2PtII species useful as synthons for generation of various (aminocarbene)Pt II complexes. *J. Chem. Crystallogr.* **2012**, *42*, 1170–1175. [CrossRef]
29. Mikhaylov, V.N.; Sorokoumov, V.N.; Novikov, A.S.; Melnik, M.V.; Tskhovrebov, A.G.; Balova, I.A. Intramolecular hydrogen bonding stabilizes trans-configuration in a mixed carbene/isocyanide PdII complexes. *J. Organomet. Chem.* **2020**, *912*, 121174. [CrossRef]
30. Grudova, M.V.; Kubasov, A.S.; Tskhovrebov, A.G. Synthesis and Crystal Structure of the Dirhodium Tetraacetate-Di(Cyclohexylisocyanide) Complex. *J. Struct. Chem.* **2021**, *62*, 1795–1800. [CrossRef]
31. Buslov, I.V.; Novikov, A.S.; Khrustalev, V.N.; Grudova, M.V.; Kubasov, A.S.; Matsulevich, Z.V.; Borisov, A.V.; Lukiyanova, J.M.; Grishina, M.M.; Kirichuk, A.A.; et al. 2-Pyridylselenenyl versus 2-Pyridyltellurenyl Halides: Symmetrical Chalcogen Bonding in the Solid State and Reactivity towards Nitriles. *Symmetry* **2021**, *13*, 2350. [CrossRef]
32. Khrustalev, V.N.; Grishina, M.M.; Matsulevich, Z.V.; Lukiyanova, J.M.; Borisova, G.N.; Osmanov, V.K.; Novikov, A.S.; Kirichuk, A.A.; Borisov, A.V.; Solari, E.; et al. Novel cationic 1,2,4-selenadiazoles: Synthesis via addition of 2-pyridylselenyl halides to unactivated nitriles, structures and four-center Se···N contacts. *Dalt. Trans.* **2021**, *50*, 10689–10691. [CrossRef]
33. Grudova, M.V.; Khrustalev, V.N.; Kubasov, A.S.; Strashnov, P.V.; Matsulevich, Z.V.; Lukiyanova, J.M.; Borisova, G.N.; Kritchenkov, A.S.; Grishina, M.M.; Artemjev, A.A.; et al. Adducts of 2-Pyridylselenenyl Halides and Nitriles as Novel Supramolecular Building Blocks: Four-Center Se···N Chalcogen Bonding versus Other Weak Interactions. *Cryst. Growth Des.* **2022**, *22*, 313–322. [CrossRef]
34. Grudova, M.V.; Kubasov, A.S.; Khrustalev, V.N.; Novikov, A.S.; Kritchenkov, A.S.; Nenajdenko, V.G.; Borisov, A.V.; Tskhovrebov, A.G. Exploring Supramolecular Assembly Space of Cationic 1,2,4-Selenodiazoles: Effect of the Substituent at the Carbon Atom and Anions. *Molecules* **2022**, *27*, 1029. [CrossRef] [PubMed]
35. Tskhovrebov, A.G.; Bokach, N.A.; Haukka, M.; Kukushkin, V.Y. Different routes for amination of platinum(II)-bound cyanoguanidine. *Inorg. Chem.* **2009**, *48*, 8678–8688. [CrossRef] [PubMed]
36. Astafiev, A.A.; Shakhov, A.M.; Kritchenkov, A.S.; Khrustalev, V.N.; Shepel, D.V.; Nadtochenko, V.A.; Tskhovrebov, A.G. Femtosecond laser synthesis of nitrogen-doped luminescent carbon dots from acetonitrile. *Dye. Pigment.* **2021**, *188*, 109176. [CrossRef]
37. Tskhovrebov, A.G.; Novikov, A.S.; Kritchenkov, A.S.; Khrustalev, V.N.; Haukka, M. Attractive halogen···halogen interactions in crystal structure of trans-dibromogold(III) complex. *Z. Für Krist. -Cryst. Mater.* **2020**, *25*, 477–480. [CrossRef]
38. Nenajdenko, V.G.; Shikhaliyev, N.G.; Maharramov, A.M.; Bagirova, K.N.; Suleymanova, G.T.; Novikov, A.S.; Khrustalev, V.N.; Tskhovrebov, A.G. Halogenated Diazabutadiene Dyes: Synthesis, Structures, Supramolecular Features, and Theoretical Studies. *Molecules* **2020**, *25*, 5013. [CrossRef] [PubMed]
39. Repina, O.V.; Novikov, A.S.; Khoroshilova, O.V.; Kritchenkov, A.S.; Vasin, A.A.; Tskhovrebov, A.G. Lasagna-like supramolecular polymers derived from the PdII osazone complexes via C(sp2)–H···Hal hydrogen bonding. *Inorg. Chim. Acta* **2020**, *502*, 119378. [CrossRef]
40. Tskhovrebov, A.G.; Vasileva, A.A.; Goddard, R.; Riedel, T.; Dyson, P.J.; Mikhaylov, V.N.; Serebryanskaya, T.V.; Sorokoumov, V.N.; Haukka, M. Palladium(II)-Stabilized Pyridine-2-Diazotates: Synthesis, Structural Characterization, and Cytotoxicity Studies. *Inorg. Chem.* **2018**, *57*, 930–934. [CrossRef]
41. Tskhovrebov, A.G.; Novikov, A.S.; Odintsova, O.V.; Mikhaylov, V.N.; Sorokoumov, V.N.; Serebryanskaya, T.V.; Starova, G.L. Supramolecular polymers derived from the PtII and PdII schiff base complexes via C(sp2)–H ... Hal hydrogen bonding: Combined experimental and theoretical study. *J. Organomet. Chem.* **2019**, *886*, 71–75. [CrossRef]
42. Tskhovrebov, A.G.; Novikov, A.S.; Tupertsev, B.S.; Nazarov, A.A.; Antonets, A.A.; Astafiev, A.A.; Kritchenkov, A.S.; Kubasov, A.S.; Nenajdenko, V.G.; Khrustalev, V.N. Azoimidazole Gold(III) Complexes: Synthesis, Structural Characterization and Self-Assembly in the Solid State. *Inorg. Chim. Acta* **2021**, *522*, 120373. [CrossRef]
43. Shikhaliyev, N.G.; Maharramov, A.M.; Bagirova, K.N.; Suleymanova, G.T.; Tsyrenova, B.D.; Nenajdenko, V.G.; Novikov, A.S.; Khrustalev, V.N.; Tskhovrebov, A.G. Supramolecular organic frameworks derived from bromoaryl-substituted dichlorodiazabutadienes via Cl···Br halogen bonding. *Mendeleev Commun.* **2021**, *31*, 191–193. [CrossRef]
44. Khrustalev, V.N.; Savchenko, A.O.; Zhukova, A.I.; Chernikova, N.Y.; Kurykin, M.A.; Novikov, A.S.; Tskhovrebov, A.G. Attractive fluorine···fluorine interactions between perfluorinated alkyl chains: A case of perfluorinated Cu(II) diiminate Cu[C2F5-C(NH)-CF=C(NH)-CF3]2. *Z. Für Krist. -Cryst. Mater.* **2021**, *236*, 117–122. [CrossRef]
45. Tskhovrebov, A.G.; Goddard, R.; Fürstner, A. Two Amphoteric Silver Carbene Clusters. *Angew. Chem. Int. Ed.* **2018**, *57*, 8089–8094. [CrossRef] [PubMed]
46. Tskhovrebov, A.G.; Lingnau, J.B.; Fürstner, A. Gold Difluorocarbenoid Complexes: Spectroscopic and Chemical Profiling. *Angew. Chem.-Int. Ed.* **2019**, *58*, 8834–8838. [CrossRef]
47. Alvarez, S. A cartography of the van der Waals territories. *Dalt. Trans.* **2013**, *42*, 8617–8636. [CrossRef]
48. Bader, R.F.W. A Quantum Theory of Molecular Structure and Its Applications. *Chem. Rev.* **1991**, *91*, 893–928. [CrossRef]
49. Andrusenko, E.V.; Kabin, E.V.; Novikov, A.S.; Bokach, N.A.; Starova, G.L.; Kukushkin, V.Y. Metal-mediated generation of triazapentadienate-terminated di- and trinuclear μ2-pyrazolate NiII species and control of their nuclearity. *New J. Chem.* **2017**, *41*, 316–325. [CrossRef]
50. Novikov, A.S. Strong metallophilic interactions in nickel coordination compounds. *Inorg. Chim. Acta* **2018**, *483*, 21–25. [CrossRef]

51. Bikbaeva, Z.M.; Novikov, A.S.; Suslonov, V.V.; Bokach, N.A.; Kukushkin, V.Y. Metal-mediated reactions between dialkylcyanamides and acetamidoxime generate unusual (nitrosoguanidinate)nickel(ii) complexes. *Dalt. Trans.* **2017**, *46*, 10090–10101. [CrossRef]
52. Shmelev, N.Y.; Okubazghi, T.H.; Abramov, P.A.; Komarov, V.Y.; Rakhmanova, M.I.; Novikov, A.S.; Gushchin, A.L. Intramolecular aurophilic interactions in dinuclear gold(i) complexes with twisted bridging 2,2′-bipyridine ligands. *Dalt. Trans.* **2021**, *50*, 12448–12456. [CrossRef]
53. Espinosa, E.; Alkorta, I.; Elguero, J.; Molins, E. From weak to strong interactions: A comprehensive analysis of the topological and energetic properties of the electron density distribution involving X-H· · · F-Y systems. *J. Chem. Phys.* **2002**, *117*, 5529–5542. [CrossRef]
54. Johnson, E.R.; Keinan, S.; Mori-Sánchez, P.; Contreras-García, J.; Cohen, A.J.; Yang, W. Revealing noncovalent interactions. *J. Am. Chem. Soc.* **2010**, *132*, 6498–6506. [CrossRef] [PubMed]
55. Contreras-García, J.; Johnson, E.R.; Keinan, S.; Chaudret, R.; Piquemal, J.-P.; Beratan, D.N.; Yang, W. NCIPLOT: A Program for Plotting Noncovalent Interaction Regions. *J. Chem. Theory Comput.* **2011**, *7*, 625–632. [CrossRef]
56. Espinosa, E.; Molins, E.; Lecomte, C. Hydrogen bond strengths revealed by topological analyses of experimentally observed electron densities. *Chem. Phys. Lett.* **1998**, *285*, 170–173. [CrossRef]
57. Bruker. *SAINT*; Bruker AXS Inc.: Madison, WI, USA, 2018.
58. Krause, L.; Herbst-Irmer, R.; Sheldrick, G.M.; Stalke, D. Comparison of silver and molybdenum microfocus X-ray sources for single-crystal structure determination. *J. Appl. Crystallogr.* **2015**, *48*, 3–10. [CrossRef] [PubMed]
59. Sheldrick, G.M. Crystal structure refinement with SHELXL. *Acta Crystallogr. Sect. C Struct. Chem.* **2015**, *71*, 3–8. [CrossRef]
60. Dolomanov, O.V.; Bourhis, L.J.; Gildea, R.J.; Howard, J.A.K.; Puschmann, H. OLEX2: A complete structure solution, refinement and analysis program. *J. Appl. Crystallogr.* **2009**, *42*, 339–341. [CrossRef]